

Dynamic analysis of coupled train - ladder track - elevated bridge system

He Xia^{*1,2}, Yushu Deng^{1,2,3}, Chaoyi Xia^{1,2}, G. De Roeck², Lin Qi⁴ and Lu Sun⁵

¹School of Civil Engineering, Beijing Jiaotong University, Beijing 100044, China

²Department of Civil Engineering, KU Leuven, B 3001 Leuven, Belgium

³CCCC Railway Consultants Co. Ltd., Beijing, China

⁴TESS Corporation Ltd., Tokyo, Japan

⁵School of Transportation, Southeast University, Nanjing 210018, China

(Received December 14, 2012, Revised July 16, 2013, Accepted August 16, 2013)

Abstract. As a new type of vibration reduction, the ladder track system has been successfully used in engineering. In this paper, a numerical model of the train-track-viaduct system is established to study the dynamic responses of an elevated bridge with ladder track. The system is composed of a vehicle submodel, a track submodel and a bridge submodel, with the measured track irregularities as the system self-excitation. The whole time histories of a train running through an elevated bridge with 3×27m continuous PC box girders are simulated. The dynamic responses of the bridge such as deflections, lateral and vertical accelerations, and the vehicle responses such as derailment factors, offload factors and car-body accelerations are calculated. The calculated results are partly validated through the comparison with the experimental data. Compared to the common slab track, adapting the ladder sleeper can effectively reduce the accelerations of the bridge girder, and also reduce the car-body accelerations and offload factors of the train vehicle.

Keywords: ladder track; elevated bridge; vibration isolation; numerical simulation; dynamic response

1. Introduction

The emergence and development of elevated rail transit has delivered us a rapid and convenient traffic medium, while at the same time caused some new problems. Since the elevated rail transit systems run in urban regions, and often through city downtowns and residential areas, they may induce serious environmental vibrations and noises (Takemiya and Bian 2007, Lombaert and Degrande 2009). In recent years, the consideration of the environmental influences of traffic-borne vibrations becomes more and more important in designing and planning traffic systems (Xia *et al.* 2007). Problems concerning the vibration influence of elevated railway and rail transit system on the environment have been considered by Chen *et al.* (2007), Andersen *et al.* (2007), Ju and Lin (2008), He *et al.* (2010), Kawatani *et al.* (2010), Yang and Yau (2011).

The dynamic behavior of railway bridges subjected to moving trainloads is one of the important problems in bridge design and maintenance. Fundamental theories for the dynamics of bridge structures under moving trains have been developed by a number of researchers, such as the

*Corresponding author, Professor, E-mail: hxia88@163.com

analytical solutions by Frýba (1999), Yau and Frýba (2007), Xia *et al.* (2011), and the stochastic solutions by Li and Zhu (2010). Numerical models of coupled train-bridge dynamic systems together with experimental validations and engineering applications in high-speed railways and elevated urban rail transits have been studied by Tanabe *et al.* (2003), Yang and Lin (2005), Wang *et al.* (2010), Martínez-Rodrigo (2010), Yang *et al.* (2010), Au *et al.* (2011), Shih *et al.* (2011), Romero *et al.* (2012), Rezvani *et al.* (2013), Guo *et al.* (2013), Zhai *et al.* (2013a, b) among others. Based on these studies, the vertical and lateral dynamic responses of bridge structures, and the safety and stability of train vehicles during transit, have been studied and many useful results were obtained and reported. However, most of the studies were carried out for structures with common tracks, whereas little research has been done for structures with vibration mitigation tracks.

Many kinds of reduction measures have been studied for railway tracks in China and abroad, such as the floating slab track (Hussein *et al.* 2006, Hui and Ng 2009), the ballast mats (Alves Costa *et al.* 2012), the isolated track (Guigou-Carter *et al.* 2006, Auersch 2008), the tuned mass dampers (Wang *et al.* 2003), and others (Xin and Gao 2011, Galvín *et al.* 2010). The effects of these isolation measures have been studied by theoretical analysis, numerical calculations and field experiments. The ladder track, as a new reduction track which has been used in Japan and America, is one of them (Wakui and Matsumoto 2002, Tahira and Miyahara 2003). Several theoretical analyses and engineering applications proved that the ladder track system, with properties of light-weight, sufficient and effective elasticity, low maintenance and low cost, is an ideal track system that can effectively reduce vibration and noise of the track while keeping good train running safety and stability (Wakui *et al.* 2002, Okuda *et al.* 2003, Xia *et al.* 2010).

In this paper, a dynamic analysis model is developed for the coupled train, ladder track and elevated bridge system, based on the authors' previous work (Xia *et al.* 2010, 2011). The train-track-bridge model is composed of the vehicle submodel with each 2-bogie 4-axle vehicle 27-DOFs, the ladder track submodel with rails, fasteners, ladder sleeper and elastic isolators, and the bridge submodel with girders, piers and foundations. By applying the measured track irregularities as the self-excitations for the train-track-bridge system, the equations of motion are established and a computer code is developed. The proposed framework is then applied to a real elevated bridge with 3×27 m continuous PC girders. The full time histories of the train traversing the bridge are simulated, from which the dynamic responses of the vehicle, the ladder track and the bridge are obtained and discussed.

2. Elastically-supported ladder track system

The Elastically-supported ladder track is a new type of low-noise and low-vibration track system, which consists of ladder sleepers, L-shaped reinforced concrete bases, resilient isolators and buffer pads made of polyurethane damping materials. The ladder sleeper, as shown in Fig. 1, is a ladder-shaped structure consisting of twin longitudinal PC beams and transverse steel-pipe connectors. The transverse steel-pipe connectors are rigidly connected with the longitudinal beams, which ensure the required track-gauge.

The ladder sleeper is supported through the resilient isolators and the transverse buffer-pads by the L-shaped RC bases to reduce the vibration spreading on the bridge girder and to mitigate the structure noise, as shown in Fig. 2. The transverse buffer-pads are also meant for keeping the transverse stability of the sleeper. The longitudinal forces of the sleeper are resisted by the slots on the vertical arms of the L-shaped RC bases, through the convex stoppers on the longitudinal beams

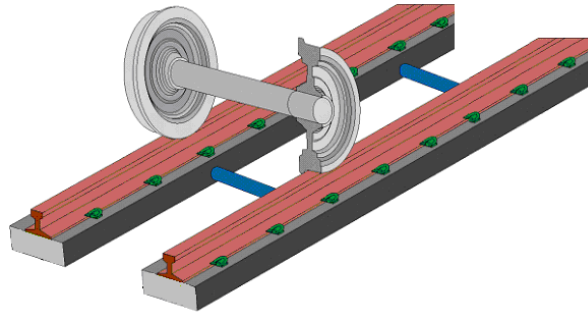


Fig. 1 Ladder sleeper with longitudinal PC beams and steel-pipe connectors

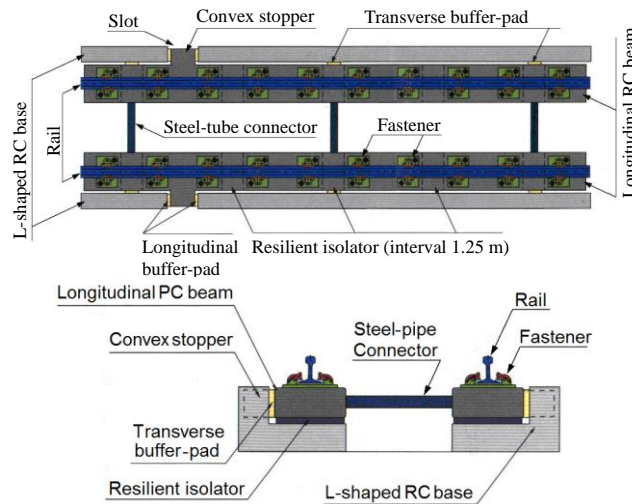


Fig. 2 Formation of the elastically-supported ladder track system

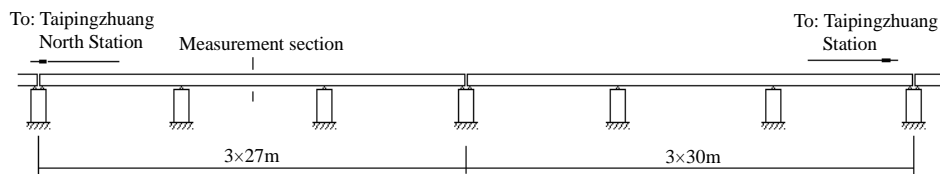


Fig. 3 The trial section of elevated bridge with ladder track on Metro Line 5 in Beijing

and longitudinal buffer-pads, to prevent the sleepers from creeping. The longitudinal PC beams can be regarded as the secondary longitudinal beams in addition to the rails, thus the rails together with the longitudinal PC beams are bearing the train load, so forming a composite track with high stiffness, and thus increasing the performance of load dispersion (Deng *et al.* 2007).

The ladder track system has been successfully used in several subways and elevated bridges in Japan and has been installed in trial sections in America. In China, a ladder track trial section with a full length of 171 m has been established on the elevated bridge of the Beijing Metro Line 5. The trial section crosses two straight lined continuous PC box girders, with a 3x30m span and a 3x27m span, as shown in Fig. 3. On the bridge, the down-line (to the Taipingzhuang North Station) adopts



Fig. 4 The ladder track on the elevated bridge (the other line is common slab track)

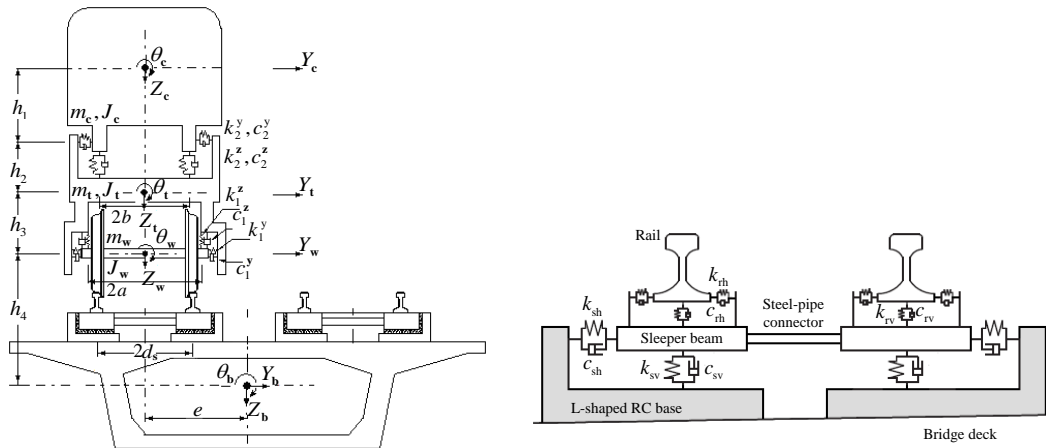


Fig. 5 The train-ladder track-bridge system model

the common slab track, and the up-line (to the Taipingzhuang Station) adopts the ladder track, as shown in Fig. 4.

3. Dynamic analysis model of coupled train-ladder track-bridge system

The dynamic model for the train-track-bridge interaction is a system composed of the train submodel, the ladder track submodel and the bridge submodel, as shown in Fig. 5 (left). In the track model, the stiffness and damping of rail-pad are modeled by springs k_r and dampers c_r , and the buffer-pad and isolators of the ladder sleepers by k_s and dampers c_s , with the subscripts v and h representing the vertical and lateral direction, respectively, as shown in Fig. 5 (right). The track irregularities are considered as the internal self-excitation for the system.

3.1 Vehicle model

The vehicle model is a train composed of a series of cars. Each car is a multi-DOF (Degree-of-Freedom) vibration system composed of car-body, bogies and wheel-sets. Each car-body or bogie considers five DOFs of lateral, rolling, yawing, floating and pitching movements, and each

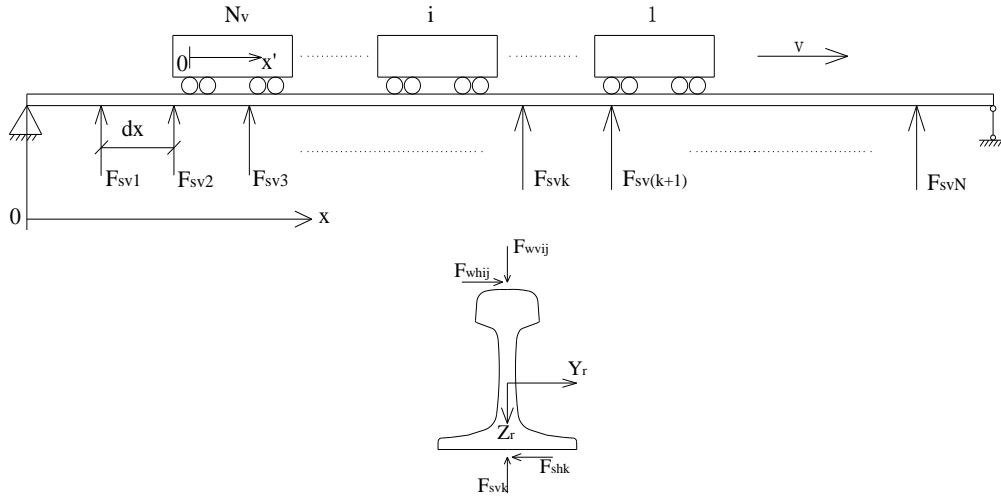


Fig. 6 Forces acting on the rail

wheel-set considers three DOFs of lateral, rolling and floating. For a rail transit car with two bogies and four wheel-sets, there are 27 DOFs considered in the calculation.

The dynamic equations of the vehicle system can be expressed in matrix form as

$$\mathbf{M}_v \ddot{\mathbf{X}}_v + \mathbf{C}_v \dot{\mathbf{X}}_v + \mathbf{K}_v \mathbf{X}_v = \mathbf{F}_v \tag{1}$$

where \mathbf{M}_v , \mathbf{C}_v and \mathbf{K}_v are the mass, damping and stiffness matrices, \mathbf{X}_v is the displacement vector, and \mathbf{F}_v the force vector acting on the train vehicles, respectively. Details of the vehicle model can be found in Xia *et al.* (2011).

3.2 Track model

For the ladder track system consisting of rails, fasteners, ladder sleeper and transverse connectors, the vibration model of the system is composed of the rail on which the train moves and the ladder sleeper with a large mass. The dynamic equations of the track system can be expressed in matrix form as

$$\mathbf{M}_t \ddot{\mathbf{X}}_t + \mathbf{C}_t \dot{\mathbf{X}}_t + \mathbf{K}_t \mathbf{X}_t = \mathbf{F}_t \tag{2}$$

where \mathbf{M}_t , \mathbf{C}_t and \mathbf{K}_t are the mass, damping and stiffness matrices, \mathbf{X}_t is the displacement vector, and \mathbf{F}_t the force vector acting on the track system, respectively.

3.2.1 Rails

The real rail is supported on sleepers via rail-pads, which is modeled as an Euler beam with infinite length discretely supported by springs and dampers. Suppose there are N_v cars moving along the rail with a speed V , the forces acting on the rail is illustrated in Fig. 6, where $o-x$ represents the rail coordinate, and $o'-x'$ the moving coordinate of the cars.

For the rail, owing to its small cross section, only the vertical and lateral movements Z_r and Y_r are considered, as shown in Fig. 6. The motion equations of them can be expressed as

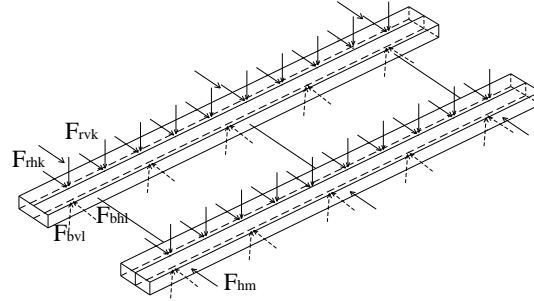


Fig. 7 Forces acting on a ladder sleeper element

$$EI_{rz} \frac{\partial^4 Z_r(x,t)}{\partial x^4} + m_r \frac{\partial^2 Z_r(x,t)}{\partial t^2} + c_r \frac{\partial Z_r(x,t)}{\partial t} = \sum_{i=1}^{N_v} \sum_{j=1}^4 F_{wvij}(t) \delta(x - x_{wij}) - \sum_{k=1}^N F_{svk}(t) \delta(x - x_k) \quad (3)$$

$$EI_{ry} \frac{\partial^4 Y_r(x,t)}{\partial x^4} + m_r \frac{\partial^2 Y_r(x,t)}{\partial t^2} + c_r \frac{\partial Y_r(x,t)}{\partial t} = \sum_{i=1}^{N_v} \sum_{j=1}^4 F_{whij}(t) \delta(x - x_{wij}) - \sum_{k=1}^N F_{shk}(t) \delta(x - x_k) \quad (4)$$

where EI_{ry} and EI_{rz} are, respectively, the vertical and lateral bending stiffnesses, m_r is the mass per unit length, and c_r is the damping coefficient of the rail; $N = N_s \times N_u$, N_s is the number of ladder sleepers considered, N_u is the number of rail-pads on each ladder sleeper; F_{wvij} and F_{whij} are, respectively, the vertical and lateral forces acting on the rail by the j -th wheel-set of the i -th car; and F_{svk} and F_{shk} are, respectively, the vertical and lateral forces reacting on the rail of the k -th rail-pad.

3.2.2 Ladder sleeper

According to its isolation principle, the ladder track belongs to two-level-isolation system: the rubber rail pad (elastic fastener) isolation between the sleeper beam and the rail, and the resilient isolator between the sleeper beam and the L-shaped base. In the analysis model, both the rubber pad and the resilient isolator are regarded as spring-damper elements. For the ladder sleeper, the two longitudinal PC beams are modeled as Euler beams in the vertical plane, while in the lateral direction the twin longitudinal PC beams and the transverse steel connectors form a frame.

Illustrated in Fig. 7 are the forces acting on the ladder sleeper. In the figure, F_{rvk} and F_{rhk} are, respectively, the vertical and lateral forces of the k -th fastener rubber pad on each longitudinal beam caused by the relative displacement between the rail and the sleeper. F_{bvl} and F_{bhl} are, respectively, the vertical and lateral forces of the l -th resilient isolator on each longitudinal beam caused by the relative displacement between the sleeper and the base (bridge deck). F_{hm} is the resistance of the m -th transverse buffer-pad caused by the lateral relative displacement between the sleeper and the base (bridge deck).

The degrees-of-freedom considered for the i -th ladder sleeper are the vertical movements of the two longitudinal beams Z_{si}^L and Z_{si}^R , the lateral movement Y_{si} and the yawing movement φ_{si} of the whole sleeper frame. Thus, the motion equations of the i -th ladder sleeper can be written as

$$E_s I_s \frac{\partial^4 Z_{si}^L(x,t)}{\partial x^4} + m_s \frac{\partial^2 Z_{si}^L(x,t)}{\partial t^2} + c_s \frac{\partial Z_{si}^L(x,t)}{\partial t} = \sum_{k=1}^{N_u} F_{rvk} \delta(x - x_{ik}) - \sum_{l=1}^{N_u} F_{bvl} \delta(x - x_{il}) \quad (5)$$

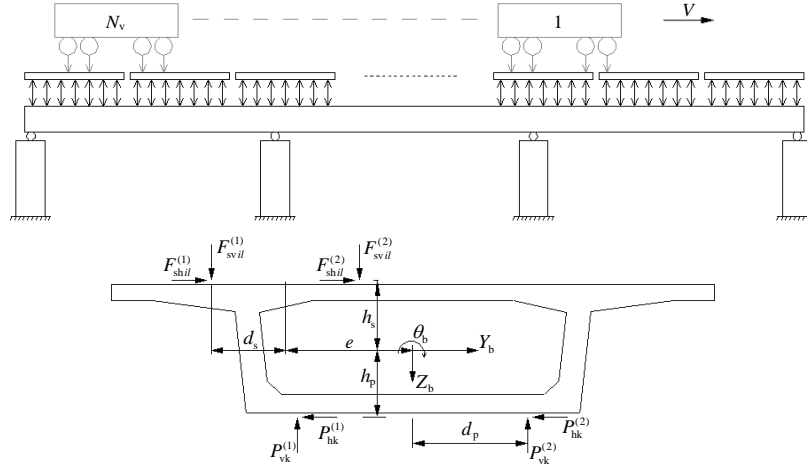


Fig. 8 Forces acting on the bridge girder

$$E_s I_s \frac{\partial^4 Z_{si}^R(x,t)}{\partial x^4} + m_s \frac{\partial^2 Z_{si}^R(x,t)}{\partial t^2} + c_s \frac{\partial Z_{si}^R(x,t)}{\partial t} = \sum_{k=1}^{N_u} F_{rvk} \delta(x - x_{ik}) - \sum_{l=1}^{N_d} F_{bvl} \delta(x - x_{il}) \quad (6)$$

$$M_s \ddot{Y}_{si} = \sum_{k=1}^{N_u} (F_{rhk}^L + F_{rhk}^R) - \sum_{l=1}^{N_d} (F_{bhl}^L + F_{bhl}^R) - \sum_{m=1}^{N_h} F_{hm} \quad (7)$$

$$J_s \ddot{\Phi}_{si} = \sum_{k=1}^{N_u} F_{rhk}^L (x_{ik} - \frac{1}{2} l_s) + \sum_{k=1}^{N_u} F_{rhk}^R (x_{ik} - \frac{1}{2} l_s) + \sum_{l=1}^{N_d} F_{bhl}^L (x_{il} - \frac{1}{2} l_s) + \sum_{l=1}^{N_d} F_{bhl}^R (x_{il} - \frac{1}{2} l_s) + \sum_{m=1}^{N_h} F_{hm}^L (x_{im} - \frac{1}{2} l_s) + \sum_{m=1}^{N_h} F_{hm}^R (x_{im} - \frac{1}{2} l_s) \quad (8)$$

where M_s , J_s and l_s are, respectively, the mass, yawing moment of inertia and length of each ladder sleeper; N_u , N_d and N_h are, respectively, the numbers of rubber pads, resilient isolators and transverse buffer-pad on each ladder sleeper.

3.3 Bridge model

Illustrated in Fig. 8 are the forces acting on the bridge girder induced by the moving train vehicles. No external forces are considered.

In the figure, F_{svil} and F_{hvil} represent, respectively, the vertical and lateral forces from the l -th isolator of the i -th sleeper on the bridge girder, which are opposite to F_{bvil} and F_{bhil} . They are expressed as follows

$$F_{svil}^{(1)} = k_{sv} \left[Z_{si}^{(1)}(x_{il}, t) - Z_b(x_{bil}, t) + (e + d_s) \theta_b \right] + c_{sv} \left[\dot{Z}_{si}^{(1)}(x_{il}, t) - \dot{Z}_b(x_{bil}, t) + (e + d_s) \dot{\theta}_b \right] \quad (9a)$$

$$F_{svil}^{(2)} = k_{sv} \left[Z_{si}^{(2)}(x_{il}, t) - Z_b(x_{bil}, t) + (e - d_s) \theta_b \right] + c_{sv} \left[\dot{Z}_{si}^{(2)}(x_{il}, t) - \dot{Z}_b(x_{bil}, t) + (e - d_s) \dot{\theta}_b \right] \quad (9b)$$

$$P_{vk}^{(1)} = k_{pv} [Z_b(x_{pk}, t) - d_p \theta_b] + c_{pv} [\dot{Z}_b(x_{pk}, t) - d_p \dot{\theta}_b] \quad (10a)$$

$$P_{vk}^{(2)} = k_{pv} [Z_b(x_{pk}, t) + d_p \theta_b] + c_{pv} [\dot{Z}_b(x_{pk}, t) + d_p \dot{\theta}_b] \quad (10b)$$

$$F_{shil}^{(1)} = k_{sh} [Y_{si}^{(1)}(x_{il}, t) + (x_{il} - 0.5l_s)\varphi_s - Y_b(x_b, t) + h_s \theta_b] \\ + c_{sh} [\dot{Y}_{si}^{(1)}(x_{il}, t) + (x_{il} - 0.5l_s)\dot{\varphi}_s - \dot{Y}_b(x_b, t) + h_s \dot{\theta}_b] \quad (11a)$$

$$F_{shil}^{(2)} = k_{sh} [Y_{si}^{(2)}(x_{il}, t) + (x_{il} - 0.5l_s)\varphi_s - Y_b(x_b, t) + h_s \theta_b] \\ + c_{sh} [\dot{Y}_{si}^{(2)}(x_{il}, t) + (x_{il} - 0.5l_s)\dot{\varphi}_s - \dot{Y}_b(x_b, t) + h_s \dot{\theta}_b] \quad (11b)$$

$$P_{hk}^{(1)} = k_{ph} [Y_b(x_b, t) - h_p \theta_b] + c_{ph} [\dot{Y}_b(x_b, t) - h_p \dot{\theta}_b] \quad (12a)$$

$$P_{hk}^{(2)} = k_{ph} [Y_b(x_b, t) + h_p \theta_b] + c_{ph} [\dot{Y}_b(x_b, t) + h_p \dot{\theta}_b] \quad (12b)$$

where k_p and c_p are the stiffness and damping coefficients of girder bearing, k_s and c_s are the stiffness and damping coefficients of buffer pad under ladder sleeper, with subscripts v and h representing the vertical and lateral direction, respectively. The other symbols can be found in the figure.

The motion equations of the bridge girder can be expressed as

$$EI_y \frac{\partial^4 Z_b(x_b, t)}{\partial x_b^4} + m_b \frac{\partial^2 Z_b(x_b, t)}{\partial t^2} + c_b \frac{\partial Z_b(x_b, t)}{\partial t} \\ = \sum_{i=1}^{N_s} \sum_{l=1}^{N_d} [F_{svil}^{(1)} \delta(x_b - x_{bil}^{(1)}) + F_{svil}^{(2)} \delta(x_b - x_{bil}^{(2)})] - \sum_{k=1}^{N_p} [P_{vk}^{(1)} \delta(x_b - x_{pk}^{(1)}) + P_{vk}^{(2)} \delta(x_b - x_{pk}^{(2)})] \quad (13)$$

$$EI_z \frac{\partial^4 Y_b(x_b, t)}{\partial x_b^4} + m_b \frac{\partial^2 Y_b(x_b, t)}{\partial t^2} + c_b \frac{\partial Y_b(x_b, t)}{\partial t} \\ = \sum_{i=1}^{N_s} \sum_{l=1}^{N_d} [F_{shil}^{(1)} \delta(x_b - x_{bil}^{(1)}) + F_{shil}^{(2)} \delta(x_b - x_{bil}^{(2)})] - \sum_{k=1}^{N_p} [P_{hk}^{(1)} \delta(x_b - x_{pk}^{(1)}) + P_{hk}^{(2)} \delta(x_b - x_{pk}^{(2)})] \quad (14)$$

$$GK \frac{\partial^4 \theta_b(x_b, t)}{\partial x_b^4} + J_b \frac{\partial^2 \theta_b(x_b, t)}{\partial t^2} + c_b \frac{\partial \theta_b(x_b, t)}{\partial t} \\ = - \sum_{i=1}^{N_s} \sum_{l=1}^{N_d} [F_{svil}^{(1)} \delta(x_b - x_{bil}^{(1)}) (d_s + e) + F_{svil}^{(2)} \delta(x_b - x_{bil}^{(2)}) e] \\ + \sum_{i=1}^{N_s} \sum_{l=1}^{N_d} [F_{shil}^{(1)} \delta(x_b - x_{bil}^{(1)}) + F_{shil}^{(2)} \delta(x_b - x_{bil}^{(2)})] h_s \\ + \sum_{k=1}^{N_p} [P_{vk}^{(1)} \delta(x_b - x_{pk}^{(1)}) - P_{vk}^{(2)} \delta(x_b - x_{pk}^{(2)})] d_p \\ + \sum_{k=1}^{N_p} [P_{hk}^{(1)} \delta(x_b - x_{pk}^{(1)}) + P_{hk}^{(2)} \delta(x_b - x_{pk}^{(2)})] h_p \quad (15)$$

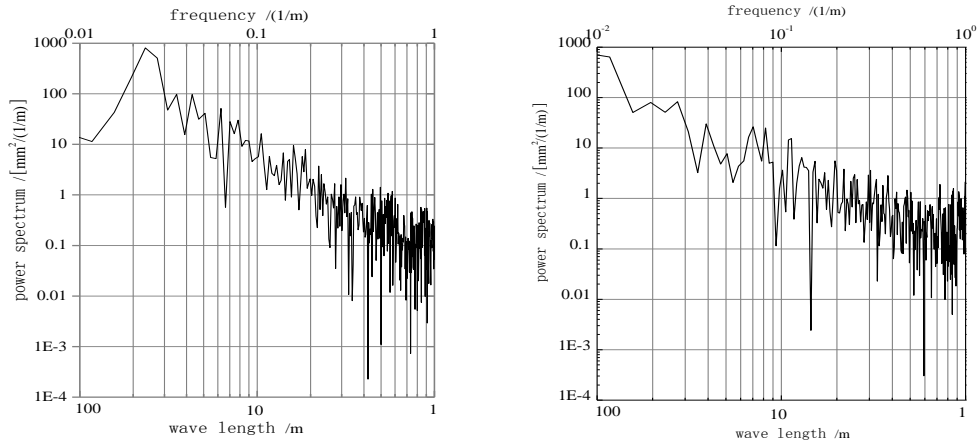


Fig. 9 Power spectra of measured vertical (left) and alignment (right) rail irregularities of ladder track

where EI_z , EI_y and GK are, respectively, the vertical, lateral and rotational stiffnesses of the girder; m_b and J_b are, respectively, the mass and rotational mass moment of inertia per unit length of the girder; c_b is the damping coefficient of the girder; N_p is the number of piers. The other symbols can be found in the figure.

The dynamic equations of the bridge can be expressed in matrix form as

$$\mathbf{M}_b \ddot{\mathbf{X}}_b + \mathbf{C}_b \dot{\mathbf{X}}_b + \mathbf{K}_b \mathbf{X}_b = \mathbf{F}_b \quad (16)$$

where \mathbf{M}_b and \mathbf{K}_b are the mass and stiffness matrices, \mathbf{X}_b is the displacement vector, and \mathbf{F}_b the force vector acting on the bridge, respectively. \mathbf{C}_b is damping matrix of the bridge structure, which is determined with Rayleigh's damping as follows (Clough and Penzien 1993)

$$\mathbf{C} = \alpha \mathbf{M} + \beta \mathbf{K} \quad (17)$$

where, α and β are coefficients for the mass matrix and stiffness matrix, respectively. When any two natural frequencies f_1 and f_2 are known, the two coefficients can be calculated by

$$\alpha = 4\pi \frac{\xi_1 f_1 f_2^2 - \xi_2 f_1^2 f_2}{f_2^2 - f_1^2}; \quad \beta = \frac{1}{\pi} \frac{\xi_2 f_2 - \xi_1 f_1}{f_2^2 - f_1^2} \quad (18)$$

where, ξ_1 and ξ_2 are damping ratios related to the two natural frequencies, which are often taken a same value in practice, namely, $\xi_1 = \xi_2$.

3.4 Track irregularities

Track irregularities refer to the deviations of the rails that support and guide the wheels from the ideal rails of perfect geometry. These irregularities are regarded as one of the main self-excitations of the interacting train-track system. A measurement was performed on the track irregularities of the ladder track and the slab track at the trial section of the Beijing Metro Line 5. The lateral and vertical track irregularities of the rails on the ladder track were measured with theodolite and level instruments, from which the vertical, alignment, rotational and gauge irregularities were obtained.

Shown in Fig. 9 are the power spectra of the vertical and alignment rail irregularities of the ladder

track. One can see that the shorter the wavelength is, the smaller the amplitude will be. Besides, the peaks in the power spectra show that there are many periodic wave components in the observed random track irregularities of this section.

3.5 Dynamic equilibrium equations for the train-track-bridge system

By combining the vehicle subsystem Eq. (1), the track subsystem Eq. (2) and the bridge subsystem Eq. (16), the dynamic equations of motion for the coupled train-track-bridge system can be obtained and expressed as

$$\begin{bmatrix} \mathbf{M}_v & \mathbf{0} & \mathbf{0} \\ \mathbf{0} & \mathbf{M}_t & \mathbf{0} \\ \mathbf{0} & \mathbf{0} & \mathbf{M}_b \end{bmatrix} \begin{bmatrix} \ddot{\mathbf{X}}_v \\ \ddot{\mathbf{X}}_t \\ \ddot{\mathbf{X}}_b \end{bmatrix} + \begin{bmatrix} \mathbf{C}_{vv} & \mathbf{C}_{vt} & \mathbf{0} \\ \mathbf{C}_{tv} & \mathbf{C}_{tt} & \mathbf{C}_{tb} \\ \mathbf{0} & \mathbf{C}_{bt} & \mathbf{C}_{bb} \end{bmatrix} \begin{bmatrix} \dot{\mathbf{X}}_v \\ \dot{\mathbf{X}}_t \\ \dot{\mathbf{X}}_b \end{bmatrix} + \begin{bmatrix} \mathbf{K}_{vv} & \mathbf{K}_{vt} & \mathbf{0} \\ \mathbf{K}_{tv} & \mathbf{K}_{tt} & \mathbf{K}_{tb} \\ \mathbf{0} & \mathbf{K}_{bt} & \mathbf{K}_{bb} \end{bmatrix} \begin{bmatrix} \mathbf{X}_v \\ \mathbf{X}_t \\ \mathbf{X}_b \end{bmatrix} = \begin{bmatrix} \mathbf{F}_{vt} \\ \mathbf{F}_{tv} + \mathbf{F}_{tb} \\ \mathbf{F}_{bt} \end{bmatrix} + \begin{bmatrix} \mathbf{F}_v^e \\ \mathbf{F}_t^e \\ \mathbf{F}_b^e \end{bmatrix} \quad (19)$$

where: \mathbf{M} , \mathbf{C} and \mathbf{K} are the mass, damping and stiffness matrices, respectively; \mathbf{X} is the displacement vector; \mathbf{F} is the force vector. The subscripts v, t and b represent the train, track and bridge, vt and tv represent the interaction between the train and the track, and bt and tb between the track and the bridge, respectively. The vector $[\mathbf{F}_v^e, \mathbf{F}_t^e, \mathbf{F}_b^e]^T$ represents the external forces acting on the train, track and bridge, respectively.

In the analysis, the track and bridge models can be established by ANSYS or other software, which are combined with the train model developed by the authors (Xia *et al.* 2011).

When the train runs on the bridge, the positions of the interacting forces between the bridge, track and train vehicles are always changing, which makes Eq. (16) become a second-order linear nonhomogeneous differential equations with time-varying coefficients. In this study, these equations are solved using the Newmark implicit step-by-step integral algorithm with $\beta=1/4$. Based on the formulation derived above, a computer code is written for the train-track-bridge system, which is used in the next case study.

4. Case study

4.1 Parameters

The case study on the dynamic responses of train-track-bridge system concerns a 3×27m elevated continuous bridge with ladder tracks. The bridge locates on the ladder track trial section of the Beijing Metro Line 5, as shown in Fig. 3. The bridge spans are PC box girders with uniform depth. The cross section and the main dimensions of the girder are shown in Fig. 10.

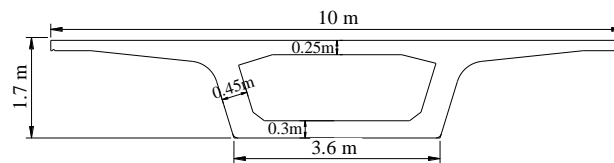


Fig. 10 Cross-section of the continuous PC box girder

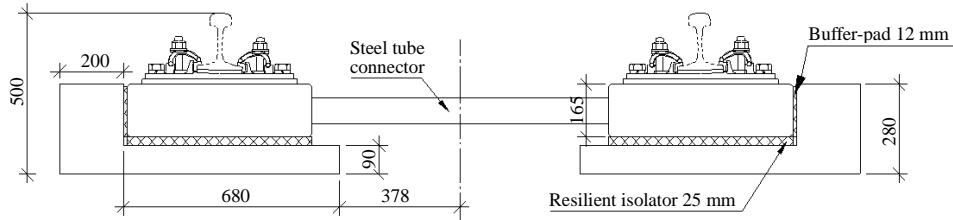


Fig. 11 Dimensions of the ladder track on the bridge (unit: mm)

Table 1 Main design parameters of the ladder track

Parameter	Resilient isolator	Transverse buffer-pad	Longitudinal buffer-pad
Stiffness /(MN/m)	17.8	42.5	25
Damping coefficient /(kNs/m)	60	80	80

Table 2 Main parameters of train vehicle.

Parameter	Value	Parameter	Value	
Full length of vehicle L /m	22.5	Mass moment of inertia of car-body /(t-m ²)	$J_{c\theta}$ 155	
Distance between two bogies $2s$ /m	15.6		$J_{c\varphi}$ 1959	
Wheel-base $2d$ /m	2.5		$J_{c\psi}$ 1875	
Mass of car body m_c /t	40.99	Mass moment of inertia of bogie /(t-m ²)	$J_{b\theta}$ 5.07	
Mass of bogie m_b /t	4.36		$J_{b\varphi}$ 1.47	
Mass of wheel-set m_w /t	1.77		$J_{b\psi}$ 3.43	
Suspension stiffness of primary spring /(kN/m)	Vertical	2976	Mass moment of inertia of wheel-set /(t-m ²)	J_w 0.92
	Lateral			20000
Suspension stiffness of secondary spring /(kN/m)	Vertical	1060	Vertical distance /m (Ref. Fig. 5)	h_2 0.36
	Lateral			460
Damping coefficient of primary dashpot /(kN.s/m)	Vertical	15		h_4 1.25
	Lateral			15
Damping coefficient of secondary dashpot /(kN.s/m)	Vertical	30	Transverse distance /m (Ref. Fig. 5)	b 1.12
	Lateral			30

The substructure of the bridge includes the concrete solid piers with rectangular section and the concrete pile foundations. The piers are 6.4 m high, and neoprene bearings are mounted on the piers to support the spans.

For the ladder track on the bridge, the main dimensions are shown in Fig. 11. The length of each track unit is 6.25 m long, and the mass is 2800 kg. The width of the longitudinal PC beam is 580 mm and the height is 165 mm. The thickness of the L-shaped RC base is 90 mm. The stiffnesses and the damping coefficients of the resilient isolators and buffer pads are listed in Table 1. During the design of the ladder track on the elevated bridge in Beijing Meitro Line 5, these dominant factors were determined via optimization by theoretical analysis and lab test (Deng *et al.* 2007).

The train consists of six vehicles, with the total length of 135 m. Each vehicle has two bogies and four axles, with the axle-weight of 132 kN, and the natural frequencies 1.04 Hz in vertical and 0.68 Hz in lateral. The other main parameters of the train vehicle are listed in Table 2.

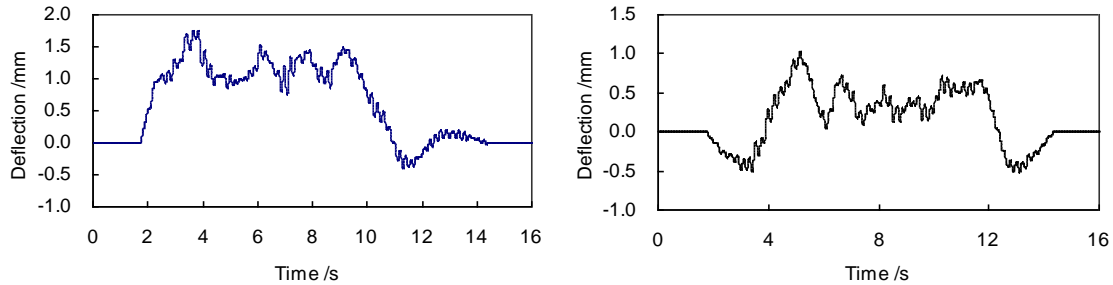


Fig. 12 Time histories of mid-span deflections of the bridge at side span (left) and middle span (right)

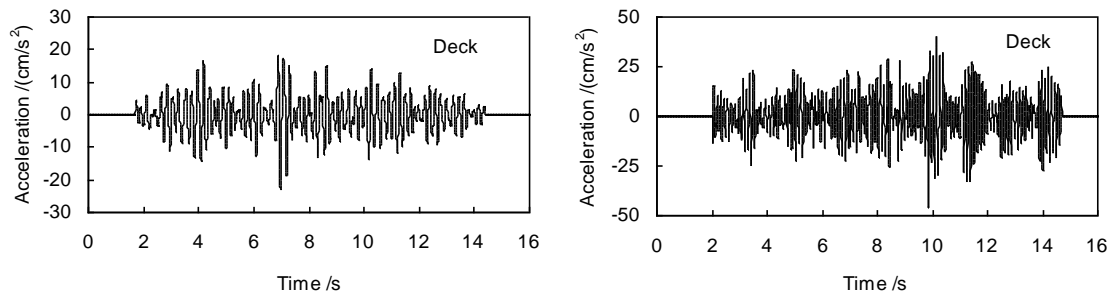


Fig. 13 Vertical (left) and lateral (right) acceleration time histories of bridge deck at side span

4.2 Calculation results

The ANSYS software was used in establishing the finite element model of the bridge, with the girders and piers being discretized by using beam elements, and the secondary loads (including track, baluster, and other facilities on the deck) of the bridge distributed on the girders as a supplementary mass.

In this analysis, the damping ratio of the bridge structure is assumed be 2%, and the two lowest natural frequencies are 4.64 Hz and 5.82 Hz, respectively, thus the Rayleigh's damping coefficients are calculated by Eq. (18) as $\alpha=0.6489$ and $\beta=6.091 \times 10^{-4}$.

According to the design train speed for the ladder track trial section of the Beijing Metro Line 5, the dynamic responses of the train-track-bridge system are calculated with the train speed range of 40-100 km/h. The integration time step is taken as 0.001s.

4.2.1 Responses of elevated bridge

Shown in Fig. 12 are the time histories of the vertical mid-span displacements of the bridge at the side span and the middle span, when the train runs on the bridge at 80 km/h. It can be seen that the vertical dynamic displacements are similar to the static influence line under a running train, and that the maximum deflections are, respectively, 1.75 mm for the side span and 1.02 mm for the middle span. This shows that the vertical deflection of the bridge under the train is mainly induced by the gravity loading of the moving train vehicles.

Shown in Fig. 13 are the vertical and lateral mid-span acceleration time histories of the bridge deck at the side span, when the train runs on the bridge at 80 km/h. It can be seen that the vertical

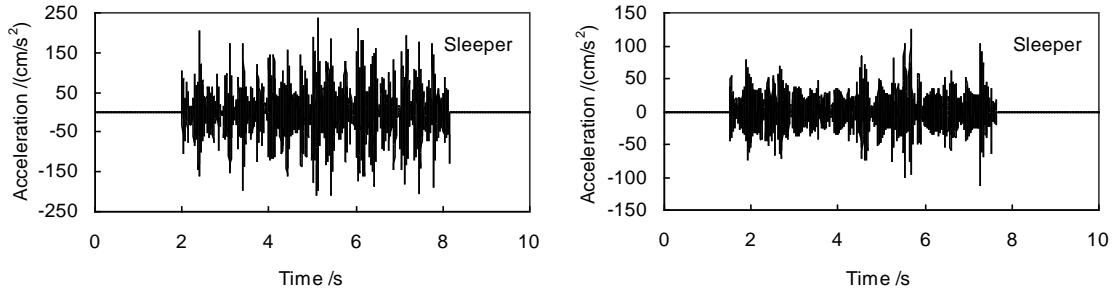


Fig. 14 Vertical (left) and lateral (right) acceleration time histories of ladder sleeper

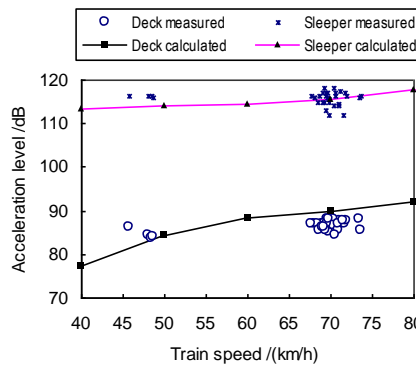


Fig. 15 Comparison of mid-span acceleration levels at ladder sleeper and bridge deck

acceleration of the bridge is bigger than the lateral one: the maximum vertical and lateral accelerations of the bridge are, respectively, 23.2 cm/s^2 and 45.06 cm/s^2 .

Shown in Fig. 14 are the acceleration histories of the sleeper at the mid-span position of the bridge. Compared to Fig. 13, one can find that the sleeper vibrates much more intensively than the bridge girder, showing a very good vibration mitigation effect.

Shown in Fig. 15 are the maximum vertical acceleration levels at the side span, when the train runs on the bridge at 40 to 80 km/h, in which the scattered symbols * and o represent, respectively, the maximum acceleration levels at the ladder sleeper and the bridge deck measured at the elevated bridge on the Beijing Metro Line 5 (Xia *et al.* 2010). The acceleration levels at the bridge deck are 25 dB to 35 dB lower than the ones at the sleeper.

To further demonstrate the vibration mitigating effect of ladder track, the maximum acceleration levels of the bridge deck when the train runs on the ladder track and the common slab track at speeds of 40 km/h to 100 km/h are calculated, as shown in Fig. 16. In the figure, the scattered symbols □ and + represent, respectively, the maximum acceleration levels of the bridge deck measured at the elevated bridge on the Beijing Metro Line 5 when the train runs on the ladder track and the common slab track (Xia *et al.* 2010). The results show that within the train speed range of 40 to 100 km/h, the maximum acceleration levels of the bridge deck increase with the train speed. When the train runs on the ladder track, the acceleration levels of the bridge deck are 6 to 10 dB lower than the train on the common slab track, showing the good vibration mitigating property of the ladder track.

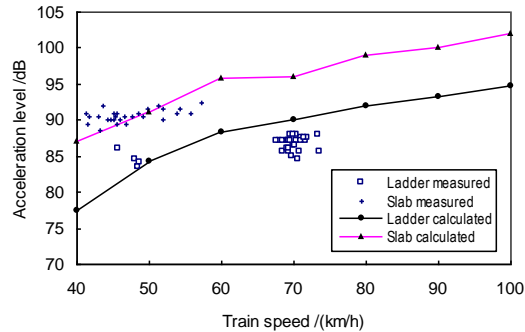


Fig. 16 Distribution of mid-span acceleration of bridge deck vs train speed

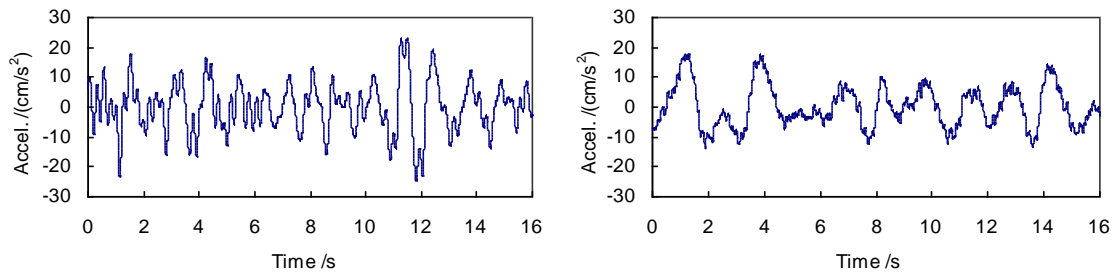


Fig. 17 Time histories of vertical (left) and lateral (right) car-body accelerations

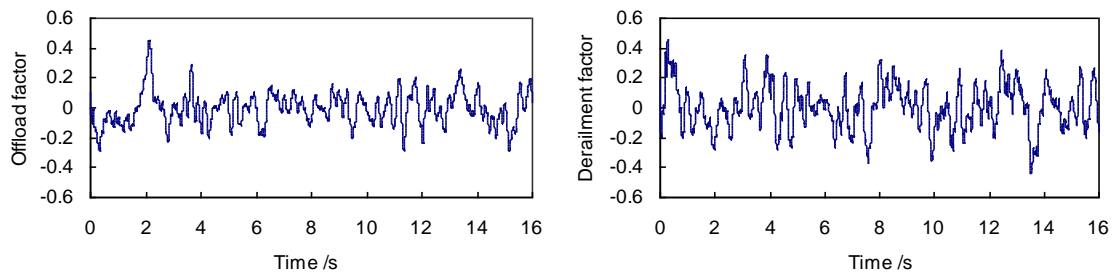


Fig. 18 Time histories of vehicle off-load factor (left) and derailment factor (right)

As the measurement site was close to the station, the train speeds were around 70 km/h on the ladder track (departing from the station) and 50 km/h on the common slab track (arriving to the station). Both Figs. 15 and 16 show a good accordance between the calculated acceleration levels and the measured data.

4.2.2 Responses of train vehicles

Shown in Fig. 17 are the time histories of the vehicle car-body accelerations when the train runs on the bridge at a speed of 80 km/h. It can be found that the vertical car-body acceleration is slightly larger than the lateral one, and has a higher frequency. The maximum accelerations are, respectively, 24.59 cm/s^2 in vertical direction and 17.88 cm/s^2 in lateral, which are well below the allowable values related to human comfort.

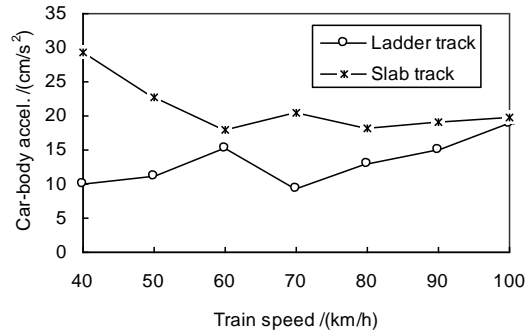


Fig. 19 Distribution of car-body acceleration vs train speed

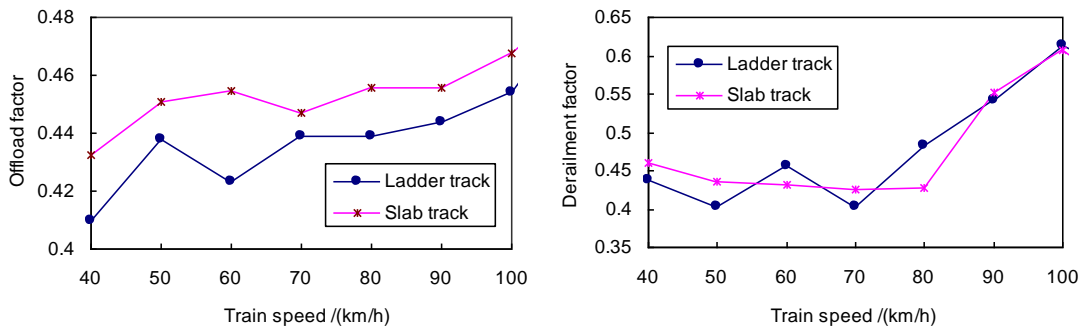


Fig. 20 Distribution of off-load factor (left) and derailment factor (right) vs train speed

There are two important evaluation indices considered for the running safety of train vehicles, which are the derailment factor Q/P (defined as the ratio of the lateral wheel-rail force to the vertical wheel-rail force) and the offload factor $\Delta P/P$ (defined as the ratio of the offload vertical wheel-rail force to the static vertical wheel-rail force). Fig. 18 shows the time histories of these two indices of a vehicle as the train runs on the ladder track of the bridge, in which the maximum offload factor is 0.45 and the maximum derailment factor is 0.493.

Shown in Figs. 19 and 20 are, respectively, the distributions of the maximum vehicle car-body accelerations, offload factors and derailment factors versus the train speed. It should be noticed that the maximum values are extracted from the corresponding whole histories of the train running through the bridge at each train speed, and normally they do not always appear at the same moment. The results show that within the train speed range of 40 to 100 km/h, the dynamic responses of train vehicles can satisfy the running safety and stability requirements. The car-body accelerations and the offload factors of the vehicle running on the ladder track are smaller than on the slab track, and the derailment factors are very similar to the ones of the slab track.

5. Conclusions

A framework for performing dynamic analysis of the coupled train, ladder-track and bridge system has been established and applied to an elevated bridge as a case study. The full time histories

of the dynamic responses for the bridge, track and train traversing the bridge have been computed with reasonable computational effort, from which the following conclusions can be drawn:

- The analysis model of train-track-bridge system can well simulate the dynamic responses of the train, ladder track and bridge, which are verified partly with the field measurement results. The proposed method is able to assess the dynamic behavior of bridges with ladder tracks and the running vehicles.

- The calculated results and the measured data show that for the bridge with ladder track, the sleeper vibrates much more intensively than the bridge girder, the acceleration levels at the deck are 25 dB to 35 dB lower than the ones at the sleeper, showing a very good vibration mitigation effect.

- Owing to the elasticity and damping effects of the resilient isolators and the transverse buffer-pads, and the good load dispersion performance of the longitudinal beams, the ladder track can effectively reduce the impact of the train loads on the bridge girder.

- The calculated results show that compared to the common slab track, adopting the ladder sleeper can also reduce the car-body accelerations and offload factors of the vehicle.

Acknowledgments

This study is sponsored by the National Key Fundamental Research Program (“973” Program, grant No. 2013CB036203), the Natural Science Foundations (U1134206, 51308035), the “111” Project (B13002) and the Fundamental Research Funds for the Central Universities (2013JBM011) of China, and the Flanders (Belgium)-China Bilateral Project (BIL 07/07).

References

- Alves Costa, P., Calçada, R. and Cardoso, A. (2012). “Ballast mats for the reduction of railway traffic vibrations, Numerical study”, *Soil Dyn. Earthq. Eng.*, 42, 137-150.
- Andersen, L., Nielsen, S. and Krenk, S. (2007), “Numerical methods for analysis of structure and ground vibration from moving loads”, *Comput. Struct.*, 85, 43-58.
- Au, F.T.K., Lou, P., Li, J., Jiang, R.J., Zhang, J., Leung, C.C.Y., Lee, P.K.K., Lee, J.H., Wong, K.Y. and Chan, H.Y. (2011), “Simulation of vibrations of Ting Kau Bridge due to vehicular loading from measurements”, *Struct. Eng. Mech.*, 40(4), 471-488.
- Auersch, L. (2008), “The effect of critically moving loads on the vibrations of soft soils and isolated railway tracks”, *J. Sound Vib.*, 310(3), 587-607.
- Chen, Y.J., Ju, S.H., Ni, S.H. and Shen, Y.J. (2007), “Prediction methodology for ground vibration induced by passing trains on bridge structures”, *J. Sound Vib.*, 302(4-5), 806-820.
- Clough, R.W. and Penzien, J. (2003), *Dynamics of Structures*, 2nd Edition, Computers & Structures Inc., Berkeley.
- Deng, Y.S., Xia, H., Zou, Y.W., Qi, L. and Inoue, H. (2007), “Dynamic action and vibration reduction design of ladder track on elevated rail transit”, *Railw. Stand. Design*, 51(10), 55-58.
- Fryba, L. (1999), *Vibration of Solids and Structures under Moving Loads*, Thomas Telford, London.
- Galvín, P., Romero, A. and Domínguez, J. (2010), “Vibrations induced by HST passage on ballast and non-ballast tracks”, *Soil Dyn. Earthq. Eng.*, 30(9), 862-873.
- Guigou-Carter, C., Villot, M., Guillerme, B. and Petit, C. (2006), “Analytical and experimental study of sleeper SAT S 312 in slab track Sateba system”, *J. Sound Vib.*, 293(3-5), 878-887.
- Guo, W.W., Xia, H. and Zhang, N. (2013), “Dynamic responses of Tsing Ma Bridge and running safety of trains subjected to Typhoon York”, *Int. J. Rail Trans.*, 1(32), 181-192.

- He, X.W., Kawatani, M. and Nishiyama, S. (2010), "An analytical approach to train-induced site vibration around Shinkansen viaducts", *Struct. Infr. Eng.*, **6**(6), 689-701.
- Hui, C.K. and Ng, C.F. (2009), "The effects of floating slab bending resonances on the vibration isolation of rail viaduct", *Applied Acoustics*, **70**(6), 830-844.
- Hussein, M.F.M. and Hunt, H.E.M. (2006), "Modeling of floating-slab tracks with continuous slabs under oscillating moving loads", *J. Sound Vib.*, **297**(1-2), 37-54.
- Ju, S.H. and Lin, H.T. (2008), "Experimentally investigating finite element accuracy for ground vibrations induced by high-speed trains", *Eng. Struct.*, **30**(3), 733-746.
- Kawatani, M., Kim, C.W. and Nishitani, K. (2010), "Assessment of traffic-induced low frequency sound radiated from a viaduct by field experiment", *Interact. Multiscale Mech.*, **3**(4), 373-388.
- Lombaert, G. and Degrande, G. (2009), "Ground-borne vibration due to static and dynamic axle loads of InterCity and high-speed trains", *J. Sound Vib.*, **319**(3-5), 1036-1066.
- Li, X.Z. and Zhu, Y. (2010), "Stochastic space vibration analysis of a train-bridge coupling system", *Interact. Multiscale Mech.*, **3**(4), 333-342.
- Martínez-Rodrigo, M.D., Lavado, J. and Museros, P. (2010), "Transverse vibrations in existing railway bridges under resonant conditions: Single-track versus double-track configurations", *Eng. Struct.*, **32**(7), 1861-1875.
- Rezvani, M.A., Vesali, F. and Eghbali, A. (2013), "Dynamic response of railway bridges traversed simultaneously by opposing moving trains", *Struc. Eng. Mech.*, **36**(5), 713-734.
- Okuda, H., Sogabe, M. and Matsumoto, N. (2003), "An environmental performance improvement of railway structural system using ladder track", *RTRI Rep.*, **17**(9), 9-14.
- Romero, A., Galvín, P. and Domínguez, J. (2012), "A time domain analysis of train induced vibrations", *Earthq. Struct.*, **3**(3), 297-313.
- Shih, H.W., Thambiratnam, D.P. and Chan, T.H.T. (2011), "Damage detection in truss bridges using vibration based multi-criteria approach", *Struc. Eng. Mech.*, **39**(2), 187-206.
- Takemiya, H. and Bian, X.C. (2007), "Shinkansen high-speed train induced ground vibrations in view of viaduct-ground interaction", *Soil Dyn. Earthq. Eng.*, **27**(6), 506-520.
- Tahira, M. and Miyahara, K. (2003), "Installation of floating ladder track on bridges", *J. Jpn. Soc. Railw. Fac.*, **6**, 448-450.
- Tanabe, M., Wakui, H., Matsumoto, N., Okuda, H., Sogabe, M. and Komiya, S. (2003), "Computational model of a Shinkansen train running on the railway structure and the industrial applications", *J. Mater. Proc. Tech.*, **140**(1-3), 705-710.
- Wakui, H., Matsumoto, N. and Okuda, H. (2002), "Structure and design of ladder sleeper", *New Railw. Struct.*, **56**(3), 26-28.
- Wakui, H. and Matsumoto, N. (2002), "Performance test of ballasted ladder track at TPCI and floating ladder track in Japan", *The 18th Transportation Research Board Annual Meeting*, Washington, USA.
- Wang, J.F., Lin, C.C. and Chen, B.L. (2003), "Vibration suppression for high-speed railway bridges using tuned mass dampers", *Int. J. Solids Struct.*, **40**(2), 465-491.
- Wang, S.Q., Xia, H., Guo, W.W. and Zhang, N. (2010), "Nonlinear dynamic response analysis of a long-span suspension bridge under running train and turbulent wind", *Interact. Multiscale Mech.*, **3**(4), 309-320.
- Xia, H., Cao, Y.M., De Roeck, G. and Degrande, G. (2007), "Environmental problems of vibrations induced by railway traffic", *Front. Arch. Civ. Eng.*, **2**, 142-152.
- Xia, H., Chen, J.G., Xia, C.Y., Inoue, H., Zenda, Y. and Qi, L. (2010), "Experimental study of train-induced structural and environmental vibrations of rail transit elevated bridge with ladder tracks", *Proc. IMechE, Part F: J. Rail Rapid Transit*, **224**(304), 115-224.
- Xia, H., De Roeck, G. and Goicolea, J.M. (2011), *Bridge vibration and controls: New Research*, Nova Science Publishers, New York.
- Xin, T. and Gao, L. (2011), "Reducing slab track vibration into bridge using elastic materials in high speed railway", *J. Sound Vib.*, **330**(10), 2237-2248.
- Yang, J.R., Li, J.Z. and Chen, Y.H. (2010), "Vibration analysis of CFST tied-arch bridge due to moving

- vehicles”, *Interact. Multiscale Mech.*, **3**(4), 389-404.
- Yang, Y.B. and Lin, C.W. (2005), “Vehicle-bridge interaction dynamics and potential applications”, *J. Sound Vib.*, 284(1-2), 205-226.
- Yang, Y.B. and Yau, J.D. (2011), “An iterative interacting method for dynamic analysis of the maglev train-guideway/ foundation-soil system”, *Eng. Struct.*, **33**(3), 1013-1024.
- Yau, J.D. and Frýba, L. (2007), “Response of suspended beams due to moving loads and vertical seismic ground excitations”, *Eng. Struct.*, **29**(12), 3255-3262.
- Zhai, W.M., Wang, S.L., Zhang, N. *et al.* (2013a), “High-speed train-track-bridge dynamic interactions -Part II: experimental validation and engineering application”, *Int. J. Rail Trans.*, **1**(1-2), 25-41.
- Zhai, W.M., Xia, H., Cai, C.B. *et al.* (2013b), “High-speed train-track-bridge dynamic interactions -Part I: theoretical model and numerical simulation”, *Int. J. Rail Trans.*, **1**(1-2), 3-24.